



Review

The Comparison of Mutational Progression in SARS-CoV-2: A Short Updated Overview

Abeer Asif ¹, Iqra Ilyas ², Mohammad Abdullah ², Sadaf Sarfraz ¹, Muhammad Mustafa ¹
and Arif Mahmood ^{3,4,*}

- ¹ KAM School of Life Science, Forman Christian College University (FCCU), Lahore 54600, Pakistan
² National Centre of Excellence in Molecular Biology (CEMB), University of The Punjab, Lahore 54590, Pakistan
³ Center for Medical Genetics and Hunan Key Laboratory of Medical Genetics, School of Life Sciences, Central South University, Changsha 410078, China
⁴ Institute of Molecular Precision Medicine, Xiangya Hospital, Central South University, Changsha 410008, China
* Correspondence: khanbiochemist007@gmail.com

Highlights:

What are the main findings?

- Understanding of mutations provides structural insight into SARS-CoV-2 variants;
- Comparison of mutations narrates the common and different mutations in the variants of concern (VOCs);
- The SD1-SD2 domain and S2 subunit provides an opportunistic spot for future virulence and vaccine development studies on SARS-CoV-2.

What is the significance of the main findings?

- The SARS-CoV-2 epidemic has paralyzed the healthcare system, shifting the focus of science. It is crucial to comprehend the mutations documented in the Beta (B.1.351), Gamma (P.1), Delta (B.1.612.2), and Omicron (B.1.1.529) variants, which will help us comprehend any future concerns related to COVID 19 and could pave the way for defense strategies against any future variants.

Abstract: The COVID-19 pandemic has impacted the world population adversely, posing a threat to human health. In the past few years, various strains of SARS-CoV-2, each with different mutations in its structure, have impacted human health in negative ways. The severe acute respiratory syndrome coronavirus 2 (SARS-CoV-2) mutations influence the virulence, antibody evasion, and Angiotensin-converting enzyme 2 (ACE2) affinity of the virus. These mutations are essential to understanding how a new strain of SARS-CoV-2 has changed and its possible effects on the human body. This review provides an insight into the spike mutations of SARS-CoV-2 variants. As the current scientific data offer a scattered outlook on the various type of mutations, we aimed to categorize the mutations of Beta (B.1.351), Gamma (P.1), Delta (B.1.612.2), and Omicron (B.1.1.529) systematically according to their location in the subunit 1 (S1) and subunit 2 (S2) domains and summarized their consequences as a result. We also compared the miscellany of mutations that have emerged in all four variants to date. The comparison shows that mutations such as D614G and N501Y have emerged in all four variants of concern and that all four variants have multiple mutations within the N-terminal domain (NTD), as in the case of the Delta variant. Other mutations are scattered in the receptor binding domain (RBD) and subdomain 2 (SD2) of the S1 domain. Mutations in RBD or NTD are often associated with antibody evasion. Few mutations lie in the S2 domain in the Beta, Gamma, and Delta variants. However, in the Omicron variant many mutations occupy the S2 domain, hinting towards a much more evasive virus.



Citation: Asif, A.; Ilyas, I.; Abdullah, M.; Sarfraz, S.; Mustafa, M.; Mahmood, A. The Comparison of Mutational Progression in SARS-CoV-2: A Short Updated Overview. *J. Mol. Pathol.* **2022**, *3*, 201–218. <https://doi.org/10.3390/jmp3040018>

Academic Editor: Giancarlo Troncone

Received: 6 September 2022

Accepted: 1 October 2022

Published: 6 October 2022

Publisher's Note: MDPI stays neutral with regard to jurisdictional claims in published maps and institutional affiliations.



Copyright: © 2022 by the authors. Licensee MDPI, Basel, Switzerland. This article is an open access article distributed under the terms and conditions of the Creative Commons Attribution (CC BY) license (<https://creativecommons.org/licenses/by/4.0/>).

Keywords: COVID-19; SARS-CoV-2 mutations; S1 domain; S2 domain; comparison of SARS-CoV-2 strains

1. Introduction

A relative of the Middle East respiratory syndrome (MERS) (2012) and severe acute respiratory syndrome SARS-CoV-2 (SARS-CoV) (2002), SARS-CoV-2 developed itself globally in 2019, targeting the respiratory system of the human body [1]. SARS-CoV-2 has attacked the human airway through various immunological and pathological pathways, leaving patients with many issues, including endothelial dysfunction, breathing problems, and possible death [2–4]. It uses the transmembrane protease serine 2 (TMPRSS2) protein, the angiotensin-converting enzyme 2, and the angiotensin-converting enzyme 2 (ACE2) receptor, located on the epithelium of the lungs, to gain entry through an endosomal route [5,6]. As shown in Figure 1, the spike protein of the virus is divided into two main domains: subunit 1 domain (S1) and subunit 2 domain (S2) [7,8]. The S2 domain mainly holds the furin cleavage site, which is a cleavage site upstream to the fusion peptide with a polybasic sequence motif (P₆₈₁ RRA₆₈₄, “PRRA”) connecting the S2 domain to the S1 domain [9].

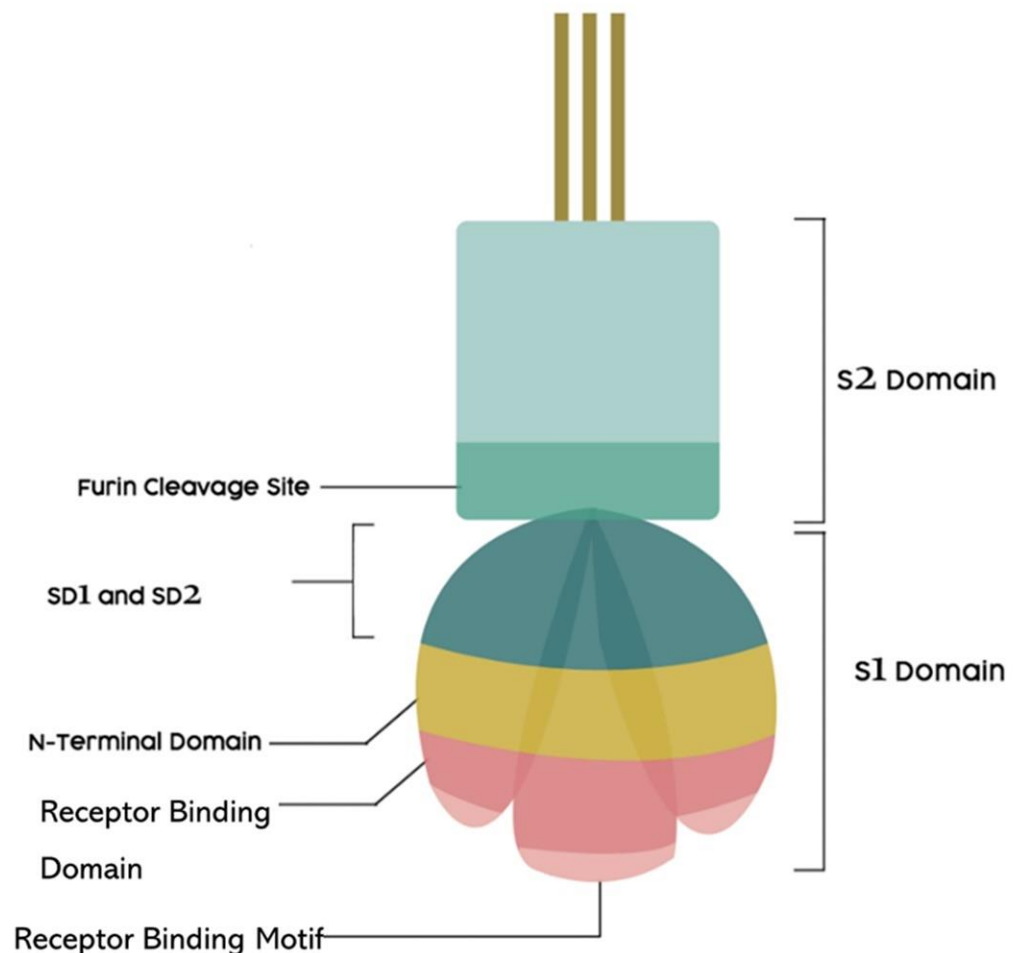


Figure 1. Details of domains in the structure of SARS-CoV-2 spike protein. The spike protein is divided into two main segments: S1 domain and S2 domain. The S1 domain essentially caps the S2 domain and is cleaved off during entry through the ACE2 receptor.

Capping the S2 subunit is the S1 subunit, which consists of S1A, S1B, S1C, and S1D [10]. The main components of the S1 domain are: the receptor binding domain (RBD), the N-terminal domain (NTD), and two central domains: SD1 and SD2 [8]. The NTD plays a crucial role in identifying certain components, such as the sialic acid carbohydrate, which enables the virus to attach to the surface of the host cell [7]. Additionally, the receptor binding motif (RBM), which interacts with the ACE2 receptor, is a component of the RBD [7]. The protease domain (PD) on the ACE2 receptor is where the (RBM) on the RBD attaches [7].

S2 is composed of a fusion peptide, a transmembrane region, two heptad repeats (HR), and an intercellular region. It consists of 3 α -helices, β -sheets, many α -helical sections, as well as α -helix and rich cysteine segments spanning the membrane [7]. After the post-fusion state, the fusion peptide allows viral membrane fusion. Without this structure, the virus would be helpless, and so, it is of significant interest in vaccine development. However, with the waxing emergence of variants, the spike protein has undergone appreciable degrees of change, which may lead to severe consequences [11]. Here, we illustrate the various mutations that have emerged in the variants of concern (VOC): Beta (B.1.351), Gamma (P.1), Delta (B.1.612.2), and Omicron (B.1.1.529) [12]. As shown in Figure 2, the mutations observed are organized according to their location on the spike protein and their summaries provided in Table 1 [13].

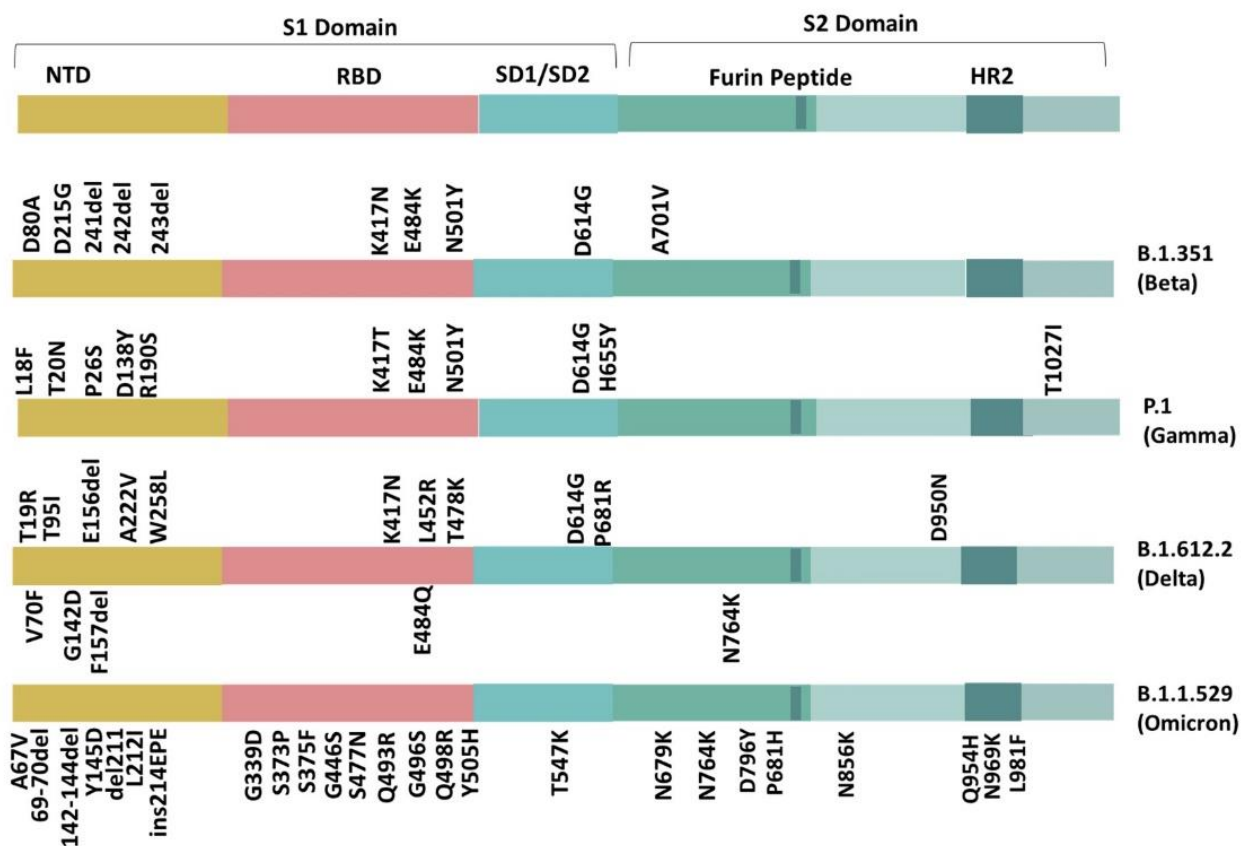


Figure 2. Mutational comparison of SARS-CoV-2 variants Beta, Gamma, Delta, and Omicron according to their regions in the S1 and S2 subunits in the spike protein.

2. Variants of SARS-CoV-2

The initial SARS-CoV-2, A.Wuhan (WH04), gave rise to Lineages A and B, with the former evolving into several contemporary variants [12,14]. South Africa reported the Beta (B.1.351) form, while Brazil and Japan highlighted the Gamma (P.1) variant. In India, the Delta (B.1.612.2) version posed a significant health crisis.

3. Identified Mutations according to Their Location in the Beta, Gamma, Delta, and Omicron Variant

3.1. S1 Domain (N-Terminal Domain (NTD))

The NTD region is known for its essential role in helping the virus attach to the surface of its host [7]. However, the NTD region is also known as a point of recognition for vaccines and the immune response, and so, most mutations in this region are expected to have a buttressing effect on viral immunity [15,16]. The following mutations have been identified in Beta, Gamma, Delta, and Omicron variant's NTDs: L18F, T19R, T20N, P26S, A67V, H69-V70 del, V70F, D80A, T95I, D138Y, del142-144, G142D, Y145D, E156- and F157- del, R158G, R190S, del211, L212I, D215G, A222V, 241/242/243 del, ins214EPE, W258L. As mentioned, some NTD mutations, such as L18F, T19R, T20N, P26S, R158G, R190S, and A222V, focus on offering immune escape to the strains they emerge in.

L18F, T20N, R190S, and P26S are in the Gamma variant. While L18F is a non-polar leucine on the 18th residue replaced by a phenylalanine, T20N has a threonine supplanted by an asparagine, and P26S has a non-polar proline replaced with a serine at the C76T gene locus. The P26S mutation occurs when a non-polar proline mutates into a polar serine. The L18F residue is buried in the folded protein and increases the escape of multiple NTD binding monoclonal antibodies, increasing the virulence of the Gamma strain [17,18]. T20N brings about the glycan shielding of supersites by glycosylation, which alters the binding capacity of antibodies, while P26S, located on the 5S glycoprotein at the C76T gene locus, brings about strong immune evasion capabilities [19,20]. R190S, with its arginine replaced by a serine, neutralizes the amino acid's polarity, affecting its interaction with the ACE2, enhancing the Gamma variant's virulence and antibody evasion further [20,21]. Lastly, A222V (alanine to valine), although seemingly inconsequential because of its transition from a non-polar amino acid to another similar amino acid, actually brings about a structural change in the inter-residual links due to the heavier valine increasing the opening of RBD, slightly increasing the viral affinity toward ACE2, but not offering much of an evasive advantage to the Delta variant [22–24]. Y145D (tyrosine to aspartic acid) and L212I (leucine to isoleucine) are two mutations found in the Omicron variant's NTD region, which reduce viral affinity to monoclonal antibodies and offer increased evasiveness [25,26]. D80A in the Beta variant's NTD region lies within the third residue of epitope RFDNPVLPF [27].

The NTD region undergoes major changes through the T19R and T95I mutation occurring in the Gamma variant, which help it increase SARS-CoV-2 virulence, while V70F, E156-, and F156- induce structural changes. Similarly, Omicron NTD mutations, such as A67V, del142-144, del211, and ins214EPE, contribute more to conformational changes, while A67V, ins214EPE, and H69-V70 also offer increased evasiveness and transmission.

T19R improves the virus' association with the ACE2 protein and helps it evade monoclonal antibodies, such as regdanvimab and bamlanivimab, by weakening their attachment to the virus [28]. T95I, a replacement of neutral and polar threonine by an acidic polar aspartic acid, has sustained itself in both the Delta and the Omicron variants. In the Delta variant, T95I works with the G142D mutation to enhance the viral load and adaptation by inducing the transition of a β -strand to an α -helix [29]. However, in the absence of T95I, the β -strand morphs into an unorganized coil at amino acid (aa) 159-165, while the aa 183-190 strand remains α -helical in shape [29]. G142D, a non-polar glycine replaced by a polar aspartic acid, produces three cardinal changes: a change in hydrogen bonding due to disparate charges, an enlarged hydrogen bonding pocket at T95I, and lastly, a transition from a Beta strand to an alpha helix at residues aa 159-167 and aa183-196 [29]. In its unmutated structure, G142 interacts with R158. However, in the Delta variant, R158G mutation induces

a steric clash, which disrupts the tightly fitted structure of SARS-CoV-2. The R158G mutates to change the hydrophilic nature of arginine to a neutral glycine and induces steric clashes with the side chain, G14D, which reduces the neutralization of monoclonal antibodies [30]. In the G142 position, the Omicron variant holds a deletion at 142-144. V70F, valine replaced by a phenylalanine, induces a change in the protein's secondary structure [31], whereas E156- and F156- deletions increase ACE2 interactions with the RBD, improving the affinity and infectivity of the Delta strain along with a possible structural alteration [32].

The H69-V70 deletion is a deletion that occurs in the apex of the helix loop motif. This out-of-frame deletion was initially recognized as a mutation located in a relatively exposed loop, which then morphs into a contracted loop, altering an antigenic site [33]. Moreover, the H69-V70 deletion follows RBM alterations, like N439K or Y453F, and increases the cleavage of S2 and embedment of the spike protein [33]. The H69-V70 deletion has also been reported to cause an increase in syncytium formation, which is often observed in severely deteriorated cases of SARS-CoV-2 patients [33]. Unlike the typical spike to ACE2 entry, syncytia formation allows a shortcut into the cell through cell-to-cell transmission [33]. Consequently, variants with the H69-V70 deletion have been observed to display higher infectivity and possibly increased pathogenicity. The 142-144 deletion also has a similar effect, increasing the immune escape, causing a shift in the N3 central loop in the supersite, and increasing infectivity [33,34]. The Y144 deletion in particular has been reported to decrease the antibody binding affinity of the virus, increasing evasion [35].

The W258L (tryptophan to leucine) mutation also expresses structural changes by skewing the R246 side chain, which results in the weakening of the interaction of antibody heavy chains with E31 and G26 as a result of the lengthened distance between the interactions [36]. Due to its unique location in the Delta strain, it offers an ill-defined area of vulnerability to antibody neutralization and demands further study to assess whether mutations within the NTD are to blame [36].

The Omicron mutations A67V, del 211, and ins214EPE also express a structural change within the SARS-CoV-2 spike protein. A67V (alanine to valine) is a mutation working with the H69-V70 deletion to induce a change in the N2 loop while also altering the antigenic site present in the wild type, possibly affecting viral infectivity [34,37]. Del 211 and ins214EPE affect the loop formed by residues 209 to 216 located next to the N4 loop in the SARS-CoV-2 spike protein [37]. Moreover, ins214EPE in combination with Y145D causes an almost 7-fold increase in resistance against the antibodies, increasing viral evasiveness [38].

Among the remaining three NTD mutations (D138Y, a neutral non-polar glycine replaced by an acidic and polar aspartic acid in the Gamma variant; D215G, a polar aspartic acid replaced by a non-polar glycine in the Beta variant; and 241-243 deletions, also in the Beta variant), there is limited information on how they influence the variant they emerge in [39]. Moreover, mutations such as D80A (aspartic acid to alanine) in the Beta variant's NTD region lie within the third residue of epitope RFDNPVLPF and have a paucity of data [27].

3.2. Receptor Binding Domain (RBD)

The RBD is the part of the SARS-CoV-2 spike protein that interacts with the ACE2 receptor. The specific segment that binds to the ACE2 receptor is the receptor binding motif (RBM) [7]. Therefore, mutations in this region may promote better interaction with ACE2, increasing stability and preventing antibody evasion.

The following mutations have been identified in the Beta, Gamma, Delta, and Omicron variant's RBD region: S371L, S373P, S375F, G339D, K417T, K417N, N440K, G446S, L452R, S477N, T478K, E484Q, E484K, E484A, Q493R, G496S, Q498R, N501Y, and Y505H.

Mutations outside the RBM region of the RBD, such as K417N/T, display increased immune escape and antibody immunization. While the K417N (lysine supplanted with a neutral, polar Asparagine) mutation appeared in the Beta, Delta, and Omicron, K417T (lysine replaced by a threonine) was found in the Gamma variant. K417N and K417T are both reported to decrease the virus' binding affinity to ACE2 [37,40]. However, when

K417N/T is in the presence of the N501Y mutation, it increases RBD's binding to the ACE2 receptor [40,41]. This allows increased viral entry and decreased antibody recognition in K417N [40,41]. This not only annihilates the antibody interaction in K417N through a 6.6-fold decrease but also interrupts the cardinal interaction that K417 held with Y52, leading to increased evasiveness of the virus [30,41–43]. For K417T, an emergence with N501Y increases the binding affinity through a four-fold increase in the interaction between ACE2 and RBD. Moreover, since K417T overlaps multiple epitopes for neutralizing various antibodies, while K417N induces viral resistance to neutralization, it needs to be monitored [19,40,44].

G339D, S317L, S373P, and S375P within the Omicron variant's RBD region are reported to improve viral evasion and increase viral affinity to ACE2. Mutations S371L (serine to leucine), S373P (serine to proline), and S375F (serine to phenylalanine) were all previously rare mutations, barely reaching 0.09% prevalence, but demonstrated a potential to provide resistance against the antibodies [45–47]. This is possibly due to the change in conformation of the antigenic site (loop connecting $\alpha 2$ and $\beta 2$), which occurred alongside an increase in ACE2 binding as a cumulative effect of these mutations [47–50]. G339D (glycine to aspartic acid) was also a previously rare mutation with a prevalence of 0.1%. However, this mutation is more associated with a slight increase in ACE2 binding and antibody evasion for monoclonal antibodies, such as sotrovimab [23,24,46].

The remaining noted RBD mutations lie within the RBM region. Mutations, such as L452R (leucine replaced by an arginine), E484Q (glutamine to glutamic acid), and T478K (uncharged Threonine to a charged Lysine), are found in the Delta variant, whereas E484K/A (glutamic acid to a lysine/alanine) and N501Y (Asparagine to a Tyrosine) occur in the Beta, Gamma, and Omicron variant of SARS-CoV-2.

L452R, E484Q, and N501Y offer increased interaction stability with the ACE2 receptor. E484Q and L452R appear together as a double variant. The original E484 located on the RBD established two hydrogen bonds with the Y53 and S56 positions on the antibody. However, with E484Q, these hydrogen bonds were disrupted, leading to a much weaker bond with the antibodies [43]. The E484Q mutation may have a weakening effect with L452R on ACE2 interaction [43]. However, many other studies argue that both point mutations individually had higher infectivity, transmission, and neutralization effects [51]. E484Q and L452R collectively induced structural changes, leading to a higher affinity with ACE2 and transmissibility due to increased S1-S2 cleavage [43]. This was also reinforced by an increased amount of bonded contact points along with a higher affinity for ACE2, which gave it a higher virulence and made neutralization difficult [51–53]. Despite their synergistic effect, they did not show any increased neutralizing activity as double mutants, apart from the initial neutralizing effect both mutations had to begin with, except for some sera [52,54]. Conclusively, E484Q is a mutation that buttresses the stability and virulence of the virus, and especially so as a double mutant with L452R in the Delta variant.

The E484 location also mutated to E484K/A. E484K is an escape mutation, as it reduces the virus's binding strength to monoclonal antibodies (convalescent and post-vaccination sera) while increasing the binding affinity toward the ACE2 receptor [55]. This change is due to salt bridge formation in commensuration to the formation of a hydrogen bond with the Glu75 residue on the ACE2 receptor [55,56], whereas E484A in the Omicron variant weakens viral affinity toward ACE2 by disrupting the necessary hydrogen bonds. However, it makes up for this by offering increased viral evasion by offsetting many other interactions with epitopes that cover the binding motif of ACE2 [37,46].

In response to the 3-fold dampening impact of the 417 mutations in both K417T and K417N forms, N501Y and E484K collaborate to cause a gain of function mutation [57]. To understand this mutation, we must first understand the set of interactions between ACE2 and SARS-CoV-2 spike protein in the form of salt bridges, non-bonded interactions, and hydrogen bonding [57]. Salt bridge formations, such as SARS2-K417 and ACE2-D30, SARS2-K458, ACE2-E23, and SARS-R403 and ACE2-E37, account for up to 40% of the total binding energies along with non-bonded interactions (Y41 and K353) with the N501

residue [57,58]. However, with the N501Y mutant, non-bonded interactions Y41, K353, and D38 come into existence along with hydrogen bonding with K353 [58]. N501Y causes a shift in its interactions, especially its salt bridges, affecting SARS2-Q498 and ACE2-Y41 by lengthening its hydrogen bond and strengthening the hydrogen bond present between SARS2-T500 and ACE2-D355 [57]. The affinity of ACE2 and SARS-CoV-2 depends on their electrostatic interactions, and so, variants with 501Y manage to bind better by a 10-fold increase and allow a stronger viral load to invade due to its decreased virus-cell dissociation [57,59]. Moreover, the N501Y mutation has reduced viral compactness, increased stability, and adapts an “open” state of perfusion, which buttresses its already increased viral entry [53,60].

The last mutation, T478K, alters the electrostatic potential, engendering a positive surface and forming salt bridges or hydrogen bonds with D38, E35, Q24, and K353 to increase the interaction between ACE2 and the spike protein [37,61]. Moreover, the longer side chain on the lysine residue engenders an increased steric hindrance whose effects are yet to be analyzed [61].

The other Omicron mutations, N440K, G446S, S477N, Q493R, G496S, and Y505H, improve SARS-CoV-2 evasiveness, while Q498R specifically strengthens viral affinity toward ACE2. While N440K (asparagine to lysine) is reported to allow viral escape against many neutralizing antibodies, G446S (glycine to serine) is more responsible for inducing steric hindrance, since, despite its low prevalence of less than 0.09%, it is in direct contact with ACE2 and reduces the activity of monoclonal antibodies (mAb), such as imdevimab and cilgavimab [23,48,49,62]. Y505H (tyrosine to histidine) of the Omicron variant has been known to improve viral escape against casirivimab, an antibody, but due to its low prevalence of 0.08% before Omicron, a paucity of data remains [23,46]. S477N (serine to asparagine), Q493R (glutamine to arginine), and G496S (glycine to serine) change the antigenic traits, offering a significant immune evasion through steric hindrance against the antibodies that bind to the RBD region [23,37,46]. In fact, S493R, Q496S, and Q498R (glutamine to arginine) in particular are reported to strengthen viral affinity toward ACE2 by 6-fold with N501Y, a previously established mutation [37,62,63].

3.3. SD1-SD2 Region

The SD1-SD2 region in the S1 spike protein subunit has been reported to act by triggering the RBD up and down movement [64]. Hydrophobic changes through mutations have also been reported to change the likelihood of RBD movement [65]. Therefore, most mutations within this region would alter how well the virus is transmitted. The following mutations have been identified in the Beta, Gamma, Delta, and Omicron variant's SD1-SD2 regions: T547K, D614G, and H655Y.

There are fewer mutations in the SD1-SD2 regions, and some have recently emerged, such as T547K (threonine to lysine), which emerged in the Omicron variant. Others, such as H655Y, have sustained themselves in both Gamma and Omicron, while the D614G (aspartic acid to glycine) mutation has survived the longest, thriving in the Beta, Gamma, Delta, and Omicron variants.

T547K increases the S1-S2 interaction between both protomers, contributing to a more compact and twisted ‘closed’ and ‘open’ structure of the spike. Moreover, although it stabilizes the “down” structure of spike protein with the help of L981F through salt bridge formation with D389, it decreases the flexibility and stability of the spike protein [66–68].

D614G and H655Y both play a part in increasing the virulence of their strain. While D614G has a direct impact on the flexibility and structure of the spike protein due to its proximity to the spike promoter, H655Y effects the charge by shifting a positive histidine to a neutral tyrosine, improving furin cleavage, antibody evasion, and viral transmission [8,44]. However, D614G does not produce such a straightforward change.

The original D614 amino acid formed salt bridges with lysine at K854 and hydrogen bonds with threonine at T859 (fusion peptide proximal region), enabling the formation of a bridge between the S1 of one protomer and the S2 of the following protomer [69]. This natural bridge shielded the S2 and furin cleavage site, reducing S1 shedding [69]. However, with the appearance of the G614 mutant, these connections appear to have been thwarted, inducing increased flexibility between the protomers and allowing the trimer to open up, expanding the contact surface of the receptor binding domain (RBD) to the ACE2 receptor [69]. Furthermore, the surface of the protomer displays a disordered loop, which appears jammed between domains, delaying the early dissociation of the S1 subunit and resulting in a more stable S trimer [70]. According to some studies, the virus may be able to use evasive mechanisms to thwart the B-immune cell response, since it is located at a B-cell epitope [30,70]. D614G operates as a double-edged sword, though, which is more plausible. The conformational shift that increased its virulence also caused a greater 1-RBD or “up” shape, increasing the exposure of the epitope and rendering it more vulnerable to neutralization [8]. It can therefore be affected by ACE2-based inhibitors and anti-SARS-CoV sera. According to a recent study, a pseudovirus exhibiting G614 was more sensitive to monoclonal antibodies directed against RBD and sera from recovering patients than its wild counterpart [30,70].

3.4. S2 Domain

Previously, the S2 subunit of the SARS-CoV-2 spike protein held relatively fewer mutations in comparison to the S1 subunit. However, Omicron did not follow this trend and seems to have had many more mutations in S2 in comparison to the older variants. The following mutations were identified in the older variants: P681R, A701V, D950N, and T1027I. Meanwhile, in the Omicron variant, the following mutations have emerged: T547K, N679K, P681H, N764K, D796Y, N856K, Q954H, N969K, and L981F.

The P681R (proline to arginine) and D950N (asparagine to aspartic acid) mutations emerged in the Delta variant, while A701V (arginine to valine) was found in the Beta and T1027I (threonine to isoleucine) in the Gamma variant.

P681R/H and A701V are near the furin cleavage site and seem to affect viral transmission in the Delta and Beta variants, respectively. P681R specifically increases the effectiveness of furin cleavage, enhancing the separation of the S1 and S2 sites and increasing the efficiency of viral entry, producing a more transmissible virus [71]. P681H (proline to histidine), appearing in the Omicron variant, is reported to improve spike cleavage using its furin-like proteases and contribute toward an adaptive immune escape. Despite increasing cleavage, some studies argue that it had a limited impact on viral entry in the previous B.1.1.7 Alpha variant and hence needs to be studied individually for its role in the Omicron variant [72–74].

A701V, on the other hand, raises the affinity of protein interactions by enhancing the spike protein’s binding affinity. Many of the mutations (N679K, P681H, N764K, D796Y, and N856K) in Omicron that appear near the furin cleavage site seem to be involved in affecting spike protein cleavability. N679K (asparagine to lysine) causes increased O-linked glycosylation on the cleavage site, which may prevent protease recognition and reduce entry through the cell surface [75]. This not only results in decreased syncytia formation and a polybasic furin cleavage site but also forces cells to enter through the endocytic route, increasing furin-regulated cleavage [76]. Moreover, N764K (asparagine to lysine) and N856K (asparagine to lysine) collectively generate two cleavage sites for SKI-1/S1P serine protease (cut envelope glycoproteins), impairing infectivity by hindering the exposure of furin peptide to allow membrane fusion [77]. However, studies report that while N764K is associated with more infectivity and processed spike, N856K actually reduces viral spike protein mediated invasion [38]. D796Y (aspartic acid to tyrosine) is known for potentially impacting protease binding while also stabilizing the trimer by increasing glycan N-linked chains with carbohydrate formed pi interactions [57,78,79].

In heptad repeat 1 (HR1), the mutations show a trend toward fusion activity and virulence. With D950N located on the HR1 in the Delta variant, its placement in the trimer interface suggests that it may play a part in changing the behavior of the spike protein [80]. Moreover, mutations, such as Q954H, N969K, and L981F, appear in the Omicron variant. While Q954H (glutamine to histidine) was expected to increase fusion activity and a six-helix bundle emergence, it was recently clarified that it reduced fusion effectiveness with N969K [38,81,82]. N969K (asparagine to lysine) not only induces reduced infectivity but is also reported to displace the HR2 (heptad repeat 2) backbone [18]. L981F (leucine to phenylalanine), on the contrary, is reported to increase syncytia formation, spike protein mediated infection, effecting ACE2 affinity and interactions between HR 1 and 2 [38,79].

The T1027I mutation replaces a polar threonine with a non-polar isoleucine [44]. It might be a factor in the Gamma variant’s trend toward enhanced virulence and diminished susceptibility to serum and monoclonal antibodies [44].

The S2 region has the D950N mutation, which also affects the Delta variants [80]. A neutral and polar Asparagine replaces the acidic and polar aspartic acid residue (D) at position 950 (N). Its particular placement in the trimer interface suggests that it may play a part in changing the behavior of the spike protein [80].

Little research has been conducted on T1027I, located on the ends in the Gamma variant. However, it may be a significant contributor toward enhanced virulence and diminished susceptibility to serum and monoclonal antibodies [44].

Table 1. Summary of mutations in major strains of SARS-CoV-2 and their subsequent effect. These color scheme indicates different regions in spike protein.

Mutation	Beta	Gamma	Delta	Omicron	Domain	Location	Mutation Effect
L18F	.	✓	.	.	S1 Domain	NTD	It hinders the binding of antibodies and increases the virulence [83].
T19R	.	.	✓	.	S1 Domain	NTD	It increases the binding of the viral particle with the ACE2 protein and increases its evasiveness against antibodies [28].
T20N	.	✓	.	.	S1 Domain	NTD	It brings about the glycan shielding of supersites through glycosylation, which alters the binding capacity of the antibodies [19].
P26S	.	✓	.	.	S1 Domain	NTD	It brings strong immune evasion [20].
A67V	.	.	.	✓	S1 Domain	NTD	It induces conformational changes within the N2 loop and enhances viral infectivity [37].
H69-V70 del	.	.	.	✓	S1 Domain	NTD	It increases viral transmission and evasiveness [33,35,84].
V70F	.	.	✓	.	S1 Domain	NTD	It tends to change the secondary structure of the protein [31].
D80A	✓	.	.	.	S1 Domain	NTD	-
T95I	.	.	✓	.	S1 Domain	NTD	Increases virulence [29].
D138Y	.	✓	.	.	S1 Domain	NTD	-

Table 1. Cont.

Mutation	Beta	Gamma	Delta	Omicron	Domain	Location	Mutation Effect
del142-144	.	.	.	✓	S1 Domain	NTD	It enhances infectivity, evasiveness, and shifts an N3 central loop [33–35].
G142D	.	.	✓	.	S1 Domain	NTD	It produces structural changes [29].
Y145D	.	.	.	✓	S1 Domain	NTD	It increases viral evasiveness and reduces neutralization antibodies' effectivity [25,38].
E156- and F157-	.	.	✓	.	S1 Domain	NTD	-
R158G	.	.	✓	.	S1 Domain	NTD	Reduces the neutralization of monoclonal antibodies [29,30].
R190S	.	✓	.	.	S1 Domain	NTD	Enhances viral immunity [20,21].
del211	.	.	.	✓	S1 Domain	NTD	It induces configurational changes [37].
L212I	.	.	.	✓	S1 Domain	NTD	It reduces the binding affinity of some monoclonal antibodies [26].
D215G	✓	.	.	.	S1 Domain	NTD	-
A222V	.	.	✓	.	S1 Domain	NTD	It increases the opening of RBD, slightly increasing ACE2 affinity, but not evasive capabilities [22–24].
241/242/243del	✓	.	.	.	S1 Domain	NTD	-
ins214EPE	.	.	.	✓	S1 Domain	NTD	It induces a structural change in the loop in the 209-216 residue and increases viral evasiveness [37].
W258L	.	.	✓	.	S1 Domain	NTD	It skews the R246 side chain [36].
G339D	.	.	.	✓	S1 Domain	RBD	It induces a slight increase in the binding affinity to ACE2 and improves virus evasion against some neutralizing antibodies [46].
S371L	.	.	.	✓	S1 Domain	RBD	It instigates a conformational change across antigenic sites, inducing antibody resistance and increasing ACE2 binding affinity [45–49]
S373P	.	.	.	✓	S1 Domain	RBD	It induces a conformational change in $\alpha 2$ and $\beta 2$ loop and antigenic site. It also causes an increase in the binding affinity to ACE2 [45–48].

Table 1. Cont.

Mutation	Beta	Gamma	Delta	Omicron	Domain	Location	Mutation Effect
S375F	.	.	.	✓	S1 Domain	RBD	It induces a change in antigenic site and improves viral evasion [46].
K417T	.	✓	.	.	S1 Domain	RBD	It increases immune escape [40,44].
K417N	✓	.	✓	.	S1 Domain	RBD	It enhances virulence and antibody immunization [41,42,47].
N440K	.	.	.	✓	S1 Domain	RBM	It increases viral evasiveness against antibodies [46,49].
G446S	.	.	.	✓	S1 Domain	RBM	It induces steric hindrance and reduces antibody activity against the virus [23,49,62].
L452R	.	.	✓	.	S1 Domain	RBM	It leads to a more stable S subunit and a higher affinity for the ACE2 receptor [43,85].
S477N	.	.	.	✓	S1 Domain	RBM	It alters the antigenic traits of the virus, improving the virus's evasion against antibodies [37].
T478K	.	.	✓	.	S1 Domain	RBM	It engenders increased steric hindrance [61].
E484Q	.	.	✓	.	S1 Domain	RBM	Increases virulence and virus stability due to disrupted hydrogen bonds [43,51].
E484K	✓	✓	.	.	S1 Domain	RBM	Enhances antibody evasion [55].
E484A	S1 Domain	RBM	It weakens the interactions with ACE2 but increases viral evasion against antibodies [37,46].
Q493R	.	.	.	✓	S1 Domain	RBM	It contributes to increased ACE2 binding affinity and immune evasion by causing steric hindrance [23,37,48,49].
G496S	.	.	.	✓	S1 Domain	RBM	It strengthens viral affinity to ACE2 and improves viral evasiveness against antibodies [37,46,62].
Q498R	S1 Domain	RBM	It improves viral affinity to ACE2 [37,48,86].
N501Y	✓	✓	.	.	S1 Domain	RBM	It increases viral affinity with ACE2 and increases viral entry into the host [57,59].

Table 1. Cont.

Mutation	Beta	Gamma	Delta	Omicron	Domain	Location	Mutation Effect
Y505H	.	.	.	✓	S1 Domain	RBM	It improves virus evasiveness against casirivimab, a monoclonal antibody [23,46].
T547K	.	.	.	✓	S1 Domain	SD1-SD2	It improves interactions between S1 and S2, destabilizes spike protein structure, and decreases spike protein flexibility [66–68].
D614G	✓	✓	✓	✓	S1 Domain	SD1-SD2	It increases virulence but also makes it increasingly susceptible to neutralization [30,70].
H655Y	.	✓	.	✓	S1 Domain	SD1-SD2	Has a positive effect on furin cleavage and enhances the transmission of the virus [44].
N679K	.	.	.	✓	S2 Domain	Near Furin Cleavage Site	It makes the furin cleavage site more polybasic and increases its cleavability [76]. It also encourages glycosylation at the cleavage site, discouraging syncytia formation [75].
P681R	.	.	✓	.	S2 Domain	Near Furin Cleavage Site	It allows a more efficient viral entry [71].
P681H	.	.	.	✓	S2 Domain	Near Furin Cleavage Site	It enhances spike cleavage, viral infection, and offers adaptive immunity but does not significantly affect virus entry [72–74].
A701V	✓	.	.	.	S2 Domain	Near Furin Cleavage Site	It boosts viral transmission and aids in viral fitness [87].
N764K	.	.	.	✓	S2 Domain	Near Furin Cleavage Site	It provides two cleavage sites for SKI-1/S1P serine protease and increases infectivity [38,77].
D796Y	.	.	.	✓	S2 Domain	Near Furin Cleavage Site	It is reported to have a potential impact on protease binding and stabilization of the spike trimer [78,79].
N856K	.	.	.	✓	S2 Domain	Near Furin Cleavage Site	It impairs infectivity and provides potential sites for cleavage for serine SKI-1/S1P protease [38,77].
D950N	.	.	✓	.	S2 Domain	HR1	Its particular placement in the trimer interface suggests that it may play a part in changing the behavior of the spike protein [80].

Table 1. Cont.

Mutation	Beta	Gamma	Delta	Omicron	Domain	Location	Mutation Effect
Q954H	.	.	.	✓	S2 Domain	HR1	It improves fusion activity and has a possible contribution toward higher infectivity [81].
N969K	.	.	.	✓	S2 Domain	HR1	It may cause a possible displacement in HR2's backbone and is reported to impair activity [18,38].
L981F	.	.	.	✓	S2 Domain	HR1	It affects the virus' binding to the ACE2 receptor and enhances viral spike protein induced infections and syncytia formation [38,79].
T1027I	.	✓	.	.	S2 Domain	Trimerization interface	It may be a significant contributor toward enhanced virulence and diminished susceptibility to serum and monoclonal antibodies [32].

4. Conclusions

The SARS-CoV-2 virus has undergone extensive mutations, giving rise to several variants, including the Beta, Gamma, Delta, and Omicron variant. The Beta, Gamma, and Delta variants of the virus are more resistant to antibodies, have an increased affinity for ACE2, and viral evasiveness against antibodies. We may infer from the current data that mutations have mostly avoided the SD2 area of the S1 domain and have accumulated primarily in the N-terminal domain. However, in the Omicron variant, this does not hold true, as many previously rare mutations emerged in the S2 region. The Omicron variant is less pathogenic, more stable due to its various structural changes, has an increased evasion against antibodies, and its spike protein 'closed' and 'open' states appear more compact and twisted [37,67,88].

The T19R, E156del/F157del, and R190S NTD alterations boost the viral particle affinity for ACE2 binding or enhance virulence (A67V, H69-V70, del142-144). While the NTD mutations, such as A67V, V70F, G142D, del 211, and ins214EPE, cause structural alterations, others, such as L18F, P26S, Y145D, R158G, and L212I, enhance antibody evasion. The receptor binding domain, the second most frequent locus for mutations, results in further modifications, which not only boost ACE2 binding (G339D, S371L, S373P, K417T, L452R, E484K/Q, and N501Y) but also antibody evasion (G339D, S375F, N440K, K417N, and K417T). The SD1–SD2 region holds few, but stronger mutations (D614G and T478K) that result in antibody evasion and effective S1/S2 cleavage (T547K).

The most common mutations are D614G and N501Y, which are present in nearly all three of the variants mentioned. Certain patterns have been consistently seen in all four variants. However, in recently emerging variants, such as Omicron, these patterns have been overturned. Therefore, additional knowledge should be attained through developments in viral biology and surveillance strategies. We believe future assessments should focus on the overall effects of such mutations on vaccine production, as well as their consequence for patients with diabetes, cardiovascular disease, and obesity.

Author Contributions: Conceptualization, I.I. and A.A.; methodology, A.A. and I.I.; validation, M.M. and S.S.; formal analysis, M.M.; writing—original draft preparation, A.A. and M.A.; writing—review and editing, A.A., I.I. and M.A.; supervision, M.M. and A.M.; project administration, A.M. All authors have read and agreed to the published version of the manuscript.

Funding: This research received no external funding.

Conflicts of Interest: The authors declare no conflict of interest.

References

1. Petrosillo, N.; Viceconte, G.; Ergonul, O.; Ippolito, G.; Petersen, E. COVID-19, SARS and MERS: Are they closely related? *Clin. Microbiol. Infect.* **2020**, *26*, 729–734. [CrossRef] [PubMed]
2. Spadaro, S.; Fogagnolo, A.; Campo, G.; Zucchetti, O.; Verri, M.; Ottaviani, I.; Tunstall, T.; Grasso, S.; Scaramuzza, V.; Murgolo, F.; et al. Markers of endothelial and epithelial pulmonary injury in mechanically ventilated COVID-19 ICU patients. *Crit. Care* **2021**, *25*, 74. [CrossRef] [PubMed]
3. Contoli, M.; Papi, A.; Tomassetti, L.; Rizzo, P.; Sega, F.V.D.; Fortini, F.; Torsani, F.; Morandi, L.; Ronzoni, L.; Zucchetti, O.; et al. Blood interferon- α levels and severity, outcomes, and inflammatory profiles in hospitalized COVID-19 patients. *Front. Immunol.* **2021**, *12*, 648004. [CrossRef] [PubMed]
4. Sega, F.V.D.; Fortini, F.; Spadaro, S.; Ronzoni, L.; Zucchetti, O.; Manfrini, M.; Mikus, E.; Fogagnolo, A.; Torsani, F.; Pavasini, R.; et al. Time course of endothelial dysfunction markers and mortality in COVID-19 patients: A pilot study. *Clin. Transl. Med.* **2021**, *11*, e283. [CrossRef]
5. Jackson, C.B.; Farzan, M.; Chen, B.; Choe, H. Mechanisms of SARS-CoV-2 entry into cells. *Nat. Rev. Mol. Cell Biol.* **2022**, *23*, 3–20. [CrossRef] [PubMed]
6. Shang, J.; Wan, Y.; Luo, C.; Ye, G.; Geng, Q.; Auerbach, A.; Li, F. Cell entry mechanisms of SARS-CoV-2. *Proc. Natl. Acad. Sci. USA* **2020**, *117*, 11727–11734. [CrossRef]
7. Mejdani, M.; Haddadi, K.; Pham, C.; Mahadevan, R. SARS-CoV-2 receptor-binding mutations and antibody contact sites. *Antib. Ther.* **2021**, *4*, 149–158. [CrossRef]
8. Weissman, D.; Alameh, M.-G.; de Silva, T.; Collini, P.; Hornsby, H.; Brown, R.; LaBranche, C.C.; Edwards, R.J.; Sutherland, L.; Santra, S.; et al. D614G spike mutation increases SARS CoV-2 susceptibility to neutralization. *Cell Host Microbe* **2021**, *29*, 23–31. [CrossRef]
9. Ou, X.; Liu, Y.; Lei, X.; Li, P.; Mi, D.; Ren, L.; Guo, L.; Guo, R.; Chen, T.; Hu, J.; et al. Characterization of spike glycoprotein of SARS-CoV-2 on virus entry and its immune cross-reactivity with SARS-CoV. *Nat. Commun.* **2020**, *11*, 1620. [CrossRef]
10. Guruprasad, K. Mutations in human SARS-CoV-2 spike proteins, potential drug binding and epitope sites for COVID-19 therapeutics development. *Curr. Res. Struct. Biol.* **2022**, *4*, 41–50. [CrossRef]
11. COVID-19 Map—Johns Hopkins Coronavirus Resource Center. 2022. Available online: <https://coronavirus.jhu.edu/map.html> (accessed on 4 August 2022).
12. Centers for Disease Control and Prevention. SARS-CoV-2 Variant Classifications and Definitions. 2019. Available online: <https://www.cdc.gov/coronavirus/2019-ncov/variants/variant-classifications.html> (accessed on 4 August 2022).
13. Peters, M.H.; Bastidas, O.; Kokron, D.S.; Henze, C.E. Static all-atom energetic mappings of the SARS-Cov-2 spike protein and dynamic stability analysis of “Up” versus “Down” protomer states. *PLoS ONE* **2020**, *15*, e0241168. [CrossRef] [PubMed]
14. Rambaut, A.; Holmes, E.C.; O’Toole, Á.; Hill, V.; McCrone, J.T.; Ruis, C.; du Plessis, L.; Pybus, O.G. A dynamic nomenclature proposal for SARS-CoV-2 lineages to assist genomic epidemiology. *Nat. Microbiol.* **2020**, *5*, 1403–1407. [CrossRef] [PubMed]
15. Yahi, N.; Chahinian, H.; Fantini, J. Infection-enhancing anti-SARS-CoV-2 antibodies recognize both the original Wuhan/D614G strain and Delta variants. A potential risk for mass vaccination? *J. Infect.* **2021**, *83*, 607–635. [CrossRef] [PubMed]
16. Kubik, S.; Arrigo, N.; Bonet, J.; Xu, Z. Mutational hotspot in the SARS-CoV-2 Spike protein N-terminal domain conferring immune escape potential. *Viruses* **2021**, *13*, 2114. [CrossRef]
17. Singh, P.; Sharma, K.; Singh, P.; Bhargava, A.; Negi, S.S.; Sharma, P.; Bhise, M.; Tripathi, M.K.; Jindal, A.; Nagarkar, N.M. Genomic characterization unravelling the causative role of SARS-CoV-2 Delta variant of lineage B. 1.617. 2 in 2nd wave of COVID-19 pandemic in Chhattisgarh, India. *Microb. Pathog.* **2022**, *164*, 105404. [CrossRef]
18. McCallum, M.; De Marco, A.; Lempp, F.A.; Tortorici, M.A.; Pinto, D.; Walls, A.C.; Beltramello, M.; Chen, A.; Liu, Z.; Zatta, F.; et al. N-terminal domain antigenic mapping reveals a site of vulnerability for SARS-CoV-2. *Cell* **2021**, *184*, 2332–2347.e16. [CrossRef]
19. Greaney, A.J.; Starr, T.N.; Gilchuk, P.; Zost, S.J.; Binshtein, E.; Loes, A.N.; Hilton, S.K.; Huddleston, J.; Eguia, R.; Crawford, K.H.; et al. Complete mapping of mutations to the SARS-CoV-2 spike receptor-binding domain that escape antibody recognition. *Cell Host Microbe* **2021**, *29*, 44–57.e9. [CrossRef]

20. Choi, H.; Chatterjee, P.; Hwang, M.; Lichtfouse, E.; Sharma, V.K.; Jinadatha, C. The viral phoenix: Enhanced infectivity and immunity evasion of SARS-CoV-2 variants. *Environ. Chem. Lett.* **2021**, *20*, 1539–1544. [[CrossRef](#)]
21. Janik, E.; Niemcewicz, M.; Podogrocki, M.; Majsterek, I.; Bijak, M. The emerging concern and interest SARS-CoV-2 variants. *Pathogens* **2021**, *10*, 633. [[CrossRef](#)]
22. Ginex, T.; Marco-Marín, C.; Wieczór, M.; Mata, C.P.; Krieger, J.; Ruiz-Rodriguez, P.; López-Redondo, M.L.; Francés-Gómez, C.; Melero, R.; Sánchez-Sorzano, C.; et al. The structural role of SARS-CoV-2 genetic background in the emergence and success of spike mutations: The case of the spike A222V mutation. *PLoS Pathog.* **2022**, *18*, e1010631. [[CrossRef](#)]
23. Alkhatib, M.; Salpini, R.; Carioti, L.; Ambrosio, F.A.; D’Anna, S.; Duca, L.; Costa, G.; Bellocchi, M.C.; Piermatteo, L.; Artese, A.; et al. Update on SARS-CoV-2 omicron variant of concern and its peculiar mutational profile. *Microbiol. Spectr.* **2022**, *10*, e02732-21. [[CrossRef](#)]
24. Cathcart, A.L.; Havenar-Daughton, C.; Lempp, F.A.; Ma, D.; Schmid, M.A.; Agostini, M.L.; Guarino, B.; Di iulio, J.; Rosen, L.E.; Tucker, H.; et al. The dual function monoclonal antibodies VIR-7831 and VIR-7832 demonstrate potent in vitro and in vivo activity against SARS-CoV-2. *BioRxiv* **2022**. in pre-print. [[CrossRef](#)]
25. Haslwanter, D.; Dieterle, M.E.; Wec, A.Z.; O’Brien, C.M.; Sakharkar, M.; Florez, C.; Tong, K.; Rappazzo, C.G.; Lasso, G.; Vergnolle, O.; et al. A combination of receptor-binding domain and N-terminal domain neutralizing antibodies limits the generation of SARS-CoV-2 spike neutralization-escape mutants. *Mbio* **2021**, *12*, e02473-21. [[CrossRef](#)] [[PubMed](#)]
26. Javanmardi, K.; Segall-Shapiro, T.H.; Chou, C.W.; Boutz, D.R.; Olsen, R.J.; Xie, X.; Xia, H.; Shi, P.Y.; Johnson, C.D.; Annapareddy, A.; et al. Antibody escape and cryptic cross-domain stabilization in the SARS-CoV-2 Omicron spike protein. *BioRxiv* **2022**. in pre-print. [[CrossRef](#)] [[PubMed](#)]
27. Redd, A.D.; Nardin, A.; Kared, H.; Bloch, E.M.; Pekosz, A.; Laeyendecker, O.; Abel, B.; Fehlings, M.; Quinn, T.C.; Tobian, A.A. CD8+ T-cell responses in COVID-19 convalescent individuals target conserved epitopes from multiple prominent SARS-CoV-2 circulating variants. *Open Forum Infect. Dis.* **2021**, *8*, ofab143. [[CrossRef](#)]
28. Das, N.C.; Chakraborty, P.; Bayry, J.; Mukherjee, S. In silico analyses on the comparative potential of therapeutic human monoclonal antibodies against newly emerged SARS-CoV-2 variants bearing mutant spike protein. *Front. Immunol.* **2021**, *12*, 782506. [[CrossRef](#)]
29. Shen, L.; Triche, T.J.; Bard, J.D.; Biegel, J.A.; Judkins, A.R.; Gai, X. Spike Protein NTD mutation G142D in SARS-CoV-2 Delta VOC lineages is associated with frequent back mutations, increased viral loads, and immune evasion. *medRxiv* **2021**. [[CrossRef](#)]
30. Kannan, S.R.; Spratt, A.N.; Cohen, A.R.; Naqvi, S.H.; Chand, H.S.; Quinn, T.P.; Lorson, C.L.; Byrareddy, S.N.; Singh, K. Evolutionary analysis of the Delta and Delta Plus variants of the SARS-CoV-2 viruses. *J. Autoimmun.* **2021**, *124*, 102715. [[CrossRef](#)]
31. Nguyen, T.T.; Pathirana, P.N.; Nguyen, T.; Nguyen, Q.V.H.; Bhatti, A.; Nguyen, D.C.; Nguyen, D.T.; Nguyen, N.D.; Creighton, D.; Abdelrazek, M. Genomic mutations and changes in protein secondary structure and solvent accessibility of SARS-CoV-2 (COVID-19 virus). *Sci. Rep.* **2021**, *11*, 3487. [[CrossRef](#)]
32. Süt, B.B. Structural analysis of novel amino acid substitutions in SARS-CoV-2 spike protein receptor-binding domain. *Hacet. J. Biol. Chem.* **2021**, *49*, 367–374. [[CrossRef](#)]
33. Meng, B.; Kemp, S.A.; Papa, G.; Datir, R.; Ferreira, I.A.; Marelli, S.; Harvey, W.T.; Lytras, S.; Mohamed, A.; Gallo, G.; et al. Recurrent emergence of SARS-CoV-2 spike deletion H69/V70 and its role in the Alpha variant B. 1.1. 7. *Cell Rep.* **2021**, *35*, 109292. [[CrossRef](#)] [[PubMed](#)]
34. Ozer, E.A.; Simons, L.M.; Adewumi, O.M.; Fowotade, A.A.; Omoruyi, E.C.; Adeniji, J.A.; Dean, T.J.; Zayas, J.; Bhimalli, P.P.; Ash, M.K.; et al. Coincident rapid expansion of two SARS-CoV-2 lineages with enhanced infectivity in Nigeria. *medRxiv* **2021**. [[CrossRef](#)]
35. McCarthy, K.R.; Rennick, L.J.; Nambulli, S.; Robinson-McCarthy, L.R.; Bain, W.G.; Haidar, G.; Duprex, W.P. Recurrent deletions in the SARS-CoV-2 spike glycoprotein drive antibody escape. *Science* **2021**, *371*, 1139–1142. [[CrossRef](#)] [[PubMed](#)]
36. McEwen, A.E.; Cohen, S.; Bryson-Cahn, C.; Liu, C.; Pergam, S.A.; Lynch, J.; Schippers, A.; Strand, K.; Whimbey, E.; Mani, N.S.; et al. Variants of concern are overrepresented among postvaccination breakthrough infections of severe acute respiratory syndrome coronavirus 2 (SARS-CoV-2) in Washington State. *Clin. Infect. Dis.* **2022**, *74*, 1089–1092. [[CrossRef](#)] [[PubMed](#)]
37. Cui, Z.; Liu, P.; Wang, N.; Wang, L.; Fan, K.; Zhu, Q.; Wang, K.; Chen, R.; Feng, R.; Jia, Z.; et al. Structural and functional characterizations of infectivity and immune evasion of SARS-CoV-2 Omicron. *Cell* **2022**, *185*, 860–871.e13. [[CrossRef](#)]
38. Pastorio, C.; Zech, F.; Noettger, S.; Jung, C.; Jacob, T.; Sanderson, T.; Sparrer, K.M.; Kirchhoff, F. Determinants of Spike infectivity, processing, and neutralization in SARS-CoV-2 Omicron subvariants BA. 1 and BA. 2. *Cell Host Microbe* **2022**, *30*, 1255–1268. [[CrossRef](#)]
39. Umair, M.; Ikram, A.; Salman, M.; Badar, N.; Haider, S.A.; Rehman, Z.; Ammar, M.; Rana, M.S.; Ali, Q. Detection and whole-genome sequencing of SARS-CoV-2 B. 1.617. 2 and B. 1.351 variants of concern from Pakistan during the COVID-19 third wave. *medRxiv* **2021**. [[CrossRef](#)]

40. Barton, M.I.; MacGowan, S.A.; Kutuzov, M.A.; Dushek, O.; Barton, G.J.; van der Merwe, P.A. Effects of common mutations in the SARS-CoV-2 Spike RBD and its ligand, the human ACE2 receptor on binding affinity and kinetics. *eLife* **2021**, *10*, e70658. [[CrossRef](#)]
41. Fratev, F. N501Y and K417N mutations in the spike protein of SARS-CoV-2 alter the interactions with Both hACE2 and human-derived antibody: A free energy of perturbation retrospective study. *J. Chem. Inf. Model.* **2021**, *61*, 6079–6084. [[CrossRef](#)]
42. Wang, R.; Zhang, Q.; Ge, J.; Ren, W.; Zhang, R.; Lan, J.; Ju, B.; Su, B.; Yu, F.; Chen, P.; et al. Analysis of SARS-CoV-2 variant mutations reveals neutralization escape mechanisms and the ability to use ACE2 receptors from additional species. *Immunity* **2021**, *54*, 1611–1621.e5. [[CrossRef](#)]
43. Cherian, S.; Potdar, V.; Jadhav, S.; Yadav, P.; Gupta, N.; Das, M.; Rakshit, P.; Singh, S.; Abraham, P.; Panda, S.; et al. SARS-CoV-2 spike mutations, L452R, T478K, E484Q and P681R, in the second wave of COVID-19 in Maharashtra, India. *Microorganisms* **2021**, *9*, 1542. [[CrossRef](#)] [[PubMed](#)]
44. Ho, D.; Wang, P.; Liu, L.; Iketani, S.; Luo, Y.; Guo, Y.; Wang, M.; Yu, J.; Zhang, B.; Kwong, P.; et al. Increased resistance of SARS-CoV-2 variants B. 1.351 and B. 1.1. 7 to antibody neutralization. *Res. Sq.* **2021**. [[CrossRef](#)]
45. Long, S.W.; Olsen, R.J.; Christensen, P.A.; Bernard, D.W.; Davis, J.J.; Shukla, M.; Nguyen, M.; Saavedra, M.O.; Yerramilli, P.; Pruitt, L.; et al. Molecular architecture of early dissemination and massive second wave of the SARS-CoV-2 virus in a major metropolitan area. *MBio* **2020**, *11*, e02707-20. [[CrossRef](#)]
46. Cao, Y.; Wang, J.; Jian, F.; Xiao, T.; Song, W.; Yisimayi, A.; Huang, W.; Li, Q.; Wang, P.; An, R.; et al. Omicron escapes the majority of existing SARS-CoV-2 neutralizing antibodies. *Nature* **2022**, *602*, 657–663. [[CrossRef](#)] [[PubMed](#)]
47. Lv, Z.; Deng, Y.-Q.; Ye, Q.; Cao, L.; Sun, C.-Y.; Fan, C.; Huang, W.; Sun, S.; Sun, Y.; Zhu, L.; et al. Structural basis for neutralization of SARS-CoV-2 and SARS-CoV by a potent therapeutic antibody. *Science* **2020**, *369*, 1505–1509. [[CrossRef](#)]
48. Kumar, S.; Thambiraja, T.S.; Karuppanan, K.; Subramaniam, G. Omicron and Delta variant of SARS-CoV-2: A comparative computational study of spike protein. *J. Med. Virol.* **2022**, *94*, 1641–1649. [[CrossRef](#)]
49. Liu, L.; Iketani, S.; Guo, Y.; Chan, J.F.-W.; Wang, M.; Liu, L.; Luo, Y.; Chu, H.; Huang, Y.; Nair, M.S.; et al. Striking antibody evasion manifested by the Omicron variant of SARS-CoV-2. *Nature* **2022**, *602*, 676–681. [[CrossRef](#)]
50. Martinez, D.R.; Schäfer, A.; Gobeil, S.; Li, D.; De la Cruz, G.; Parks, R.; Lu, X.; Barr, M.; Stalls, V.; Janowska, K.; et al. A broadly cross-reactive antibody neutralizes and protects against sarbecovirus challenge in mice. *Sci. Transl.* **2021**, *14*, eabj7125. [[CrossRef](#)]
51. Das, C.; Hazarika, P.J.; Deb, A.; Joshi, P.; Das, D.; Mattaparthi, V.S.K. Effect of double mutation (L452R and E484Q) in RBD of SPIKE Protein on its interaction with ACE2 receptor protein. *Biointerface Res. Appl. Chem.* **2022**, *13*, 97. [[CrossRef](#)]
52. Augusto, G.; Mohsen, M.O.; Zinkhan, S.; Liu, X.; Vogel, M.; Bachmann, M.F. In vitro data suggest that Indian delta variant B. 1.617 of SARS-CoV-2 escapes neutralization by both receptor affinity and immune evasion. *Allergy* **2022**, *77*, 111–117. [[CrossRef](#)]
53. Rostami, N.; Choupani, E.; Hernandez, Y.; Arab, S.S.; Jazayeri, S.M.; Gomari, M.M. SARS-CoV-2 spike evolutionary behaviors; simulation of N501Y mutation outcomes in terms of immunogenicity and structural characteristic. *J. Cell. Biochem.* **2022**, *123*, 417–430. [[CrossRef](#)] [[PubMed](#)]
54. Ferreira, I.A.T.M.; Kemp, S.A.; Datir, R.; Saito, A.; Meng, B.; Rakshit, P.; Takaori-Kondo, A.; Kosugi, Y.; Uriu, K.; Kimura, I.; et al. SARS-CoV-2 B. 1.617 mutations L452R and E484Q are not synergistic for antibody evasion. *J. Infect. Dis.* **2021**, *224*, 989–994. [[CrossRef](#)]
55. Chakraborty, S. E484K and N501Y SARS-CoV 2 spike mutants increase ACE2 recognition but reduce affinity for neutralizing antibody. *Int. Immunopharmacol.* **2022**, *102*, 108424. [[CrossRef](#)] [[PubMed](#)]
56. Yang, W.-T.; Huang, W.-H.; Liao, T.-L.; Hsiao, T.-H.; Chuang, H.-N.; Liu, P.-Y. SARS-CoV-2 E484K mutation narrative review: Epidemiology, immune escape, clinical implications, and future considerations. *Infect. Drug Resist.* **2022**, *15*, 373. [[CrossRef](#)] [[PubMed](#)]
57. Ali, F.; Kasry, A.; Amin, M. The new SARS-CoV-2 strain shows a stronger binding affinity to ACE2 due to N501Y mutant. *Med. Drug Discov.* **2021**, *10*, 100086. [[CrossRef](#)]
58. Santos, J.C.; Passos, G.A. The high infectivity of SARS-CoV-2 B. 1.1. 7 is associated with increased interaction force between Spike-ACE2 caused by the viral N501Y mutation. *BioRxiv* **2021**. in pre-print. [[CrossRef](#)]
59. Tian, F.; Tong, B.; Sun, L.; Shi, S.; Zheng, B.; Wang, Z.; Dong, X.; Zheng, P. N501Y mutation of spike protein in SARS-CoV-2 strengthens its binding to receptor ACE2. *eLife* **2021**, *10*, e69091. [[CrossRef](#)]
60. Teruel, N.; Mailhot, O.; Najmanovich, R.J. Modelling conformational state dynamics and its role on infection for SARS-CoV-2 Spike protein variants. *PLoS Comput. Biol.* **2021**, *17*, e1009286. [[CrossRef](#)]
61. Di Giacomo, S.; Mercatelli, D.; Rakhimov, A.; Giorgi, F.M. Preliminary report on severe acute respiratory syndrome coronavirus 2 (SARS-CoV-2) Spike mutation T478K. *J. Med. Virol.* **2021**, *93*, 5638–5643. [[CrossRef](#)]
62. Kannan, S.R.; Spratt, A.N.; Sharma, K.; Chand, H.S.; Byrareddy, S.N.; Singh, K. Omicron SARS-CoV-2 variant: Unique features and their impact on pre-existing antibodies. *J. Autoimmun.* **2022**, *126*, 102779. [[CrossRef](#)]

63. Zhou, D.; Dejnirattisai, W.; Supasa, P.; Liu, C.; Mentzer, A.J.; Ginn, H.M.; Zhao, Y.; Duyvesteyn, H.M.; Tuekprakhon, A.; Nutalai, R.; et al. Evidence of escape of SARS-CoV-2 variant B. 1.351 from natural and vaccine-induced sera. *Cell* **2021**, *184*, 2348–2361.e6. [[CrossRef](#)] [[PubMed](#)]
64. Berger, I.; Schaffitzel, C. The SARS-CoV-2 spike protein: Balancing stability and infectivity. *Cell Res.* **2020**, *30*, 1059–1060. [[CrossRef](#)] [[PubMed](#)]
65. Henderson, R.; Edwards, R.J.; Mansouri, K.; Janowska, K.; Stalls, V.; Gobeil, S.M.C.; Kopp, M.; Li, D.; Parks, R.; Hsu, A.L.; et al. Controlling the SARS-CoV-2 spike glycoprotein conformation. *Nat. Struct. Mol. Biol.* **2020**, *27*, 925–933. [[CrossRef](#)]
66. Al-Zyoud, W.; Haddad, H. Potential linear B-cells epitope change to a helix structure in the spike of Omicron 21L or BA. 2 predicts increased SARS-CoV-2 antibodies evasion. *Virology* **2022**, *573*, 84–95. [[CrossRef](#)] [[PubMed](#)]
67. Hong, Q.; Han, W.; Li, J.; Xu, S.; Wang, Y.; Xu, C.; Li, Z.; Wang, Y.; Zhang, C.; Huang, Z.; et al. Molecular basis of receptor binding and antibody neutralization of Omicron. *Nature* **2022**, *604*, 546–552. [[CrossRef](#)] [[PubMed](#)]
68. Zeng, C.; Evans, J.P.; Qu, P.; Faraone, J.; Zheng, Y.M.; Carlin, C.; Bednash, J.S.; Zhou, T.; Lozanski, G.; Mallampalli, R.; et al. Neutralization and stability of SARS-CoV-2 Omicron variant. *BioRxiv* **2021**, preprint. [[CrossRef](#)]
69. Ozono, S.; Zhang, Y.; Ode, H.; Sano, K.; Tan, T.S.; Imai, K.; Miyoshi, K.; Kishigami, S.; Ueno, T.; Iwatani, Y.; et al. SARS-CoV-2 D614G spike mutation increases entry efficiency with enhanced ACE2-binding affinity. *Nat. Commun.* **2021**, *12*, 848. [[CrossRef](#)]
70. Zhang, J.; Cai, Y.; Xiao, T.; Lu, J.; Peng, H.; Sterling, S.M.; Walsh, R.M., Jr.; Rits-Volloch, S.; Zhu, H.; Woosley, A.N.; et al. Structural impact on SARS-CoV-2 spike protein by D614G substitution. *Science* **2021**, *372*, 525–530. [[CrossRef](#)]
71. Liu, Y.; Liu, J.; Johnson, B.A.; Xia, H.; Ku, Z.; Schindewolf, C.; Widen, S.G.; An, Z.; Weaver, S.C.; Menachery, V.D.; et al. Delta spike P681R mutation enhances SARS-CoV-2 fitness over Alpha variant. *BioRxiv* **2021**. [[CrossRef](#)]
72. Lista, M.J.; Winstone, H.; Wilson, H.D.; Dyer, A.; Pickering, S.; Galao, R.P.; De Lorenzo, G.; Cowton, V.M.; Furnon, W.; Suarez, N.; et al. The P681H mutation in the Spike glycoprotein confers type I interferon resistance in the SARS-CoV-2 alpha (B. 1.1. 7) variant. *BioRxiv* **2021**. [[CrossRef](#)]
73. Lubinski, B.; Fernandes, M.H.; Frazier, L.; Tang, T.; Daniel, S.; Diel, D.G.; Jaimes, J.A.; Whittaker, G.R. Functional evaluation of the P681H mutation on the proteolytic activation of the SARS-CoV-2 variant B. 1.1. 7 (Alpha) spike. *iScience* **2022**, *25*, 103589. [[CrossRef](#)] [[PubMed](#)]
74. Boehm, E.; Kronig, I.; Neher, R.A.; Eckerle, I.; Vetter, P.; Kaiser, L. Novel SARS-CoV-2 variants: The pandemics within the pandemic. *Clin. Microbiol. Infect.* **2021**, *27*, 1109–1117. [[CrossRef](#)] [[PubMed](#)]
75. Lubinski, B.; Jaimes, J.A.; Whittaker, G. Intrinsic furin-mediated cleavability of the spike S1/S2 site from SARS-CoV-2 variant B. 1.529 (Omicron). *BioRxiv* **2022**. [[CrossRef](#)]
76. Maaroufi, H. The N764K and N856K mutations in SARS-CoV-2 Omicron BA. 1 S protein generate potential cleavage sites for SKI-1/S1P protease. *BioRxiv* **2022**. [[CrossRef](#)]
77. Ni, D.; Lau, K.; Turelli, P.; Raclot, C.; Beckert, B.; Nazarov, S.; Pojer, F.; Myasnikov, A.; Stahlberg, H.; Trono, D. Structural analysis of the spike of the Omicron SARS-COV-2 variant by cryo-EM and implications for immune evasion. *BioRxiv* **2021**. [[CrossRef](#)]
78. Ou, J.; Lan, W.; Wu, X.; Zhao, T.; Duan, B.; Yang, P.; Ren, Y.; Quan, L.; Zhao, W.; Seto, D.; et al. Tracking SARS-CoV-2 Omicron diverse spike gene mutations identifies multiple inter-variant recombination events. *Signal Transduct. Target. Ther.* **2022**, *7*, 138. [[CrossRef](#)]
79. Planas, D.; Veyer, D.; Baidaliuk, A.; Staropoli, I.; Guivel-Benhassine, F.; Rajah, M.M.; Planchais, C.; Porrot, F.; Robillard, N.; Puech, J.; et al. Reduced sensitivity of SARS-CoV-2 variant Delta to antibody neutralization. *Nature* **2021**, *596*, 276–280. [[CrossRef](#)]
80. Xia, S.; Liu, M.; Wang, C.; Xu, W.; Lan, Q.; Feng, S.; Qi, F.; Bao, L.; Du, L.; Liu, S.; et al. Inhibition of SARS-CoV-2 (previously 2019-nCoV) infection by a highly potent pan-coronavirus fusion inhibitor targeting its spike protein that harbors a high capacity to mediate membrane fusion. *Cell Res.* **2020**, *30*, 343–355. [[CrossRef](#)]
81. Sarkar, R.; Lo, M.; Saha, R.; Dutta, S.; Chawla-Sarkar, M. S glycoprotein diversity of the Omicron variant. *MedRxiv* **2021**. [[CrossRef](#)]
82. Yang, K.; Wang, C.; White, K.I.; Pfuetzner, R.A.; Esquivies, L.; Brunger, A.T. Structural conservation among variants of the SARS-CoV-2 spike postfusion bundle. *Proc. Natl. Acad. Sci. USA* **2022**, *119*, e2119467119. [[CrossRef](#)]
83. Kemp, S.A.; Meng, B.; Ferriera, I.A.; Datir, R.; Harvey, W.T.; Papa, G.; Lytras, S.; Collier, D.A.; Mohamed, A.; Gallo, G.; et al. Recurrent emergence and transmission of a SARS-CoV-2 spike deletion H69/V70. *BioRxiv* **2021**, *35*, 13. [[CrossRef](#)]
84. Motozono, C.; Toyoda, M.; Zahradnik, J.; Saito, A.; Nasser, H.; Tan, T.S.; Ngare, I.; Kimura, I.; Uriu, K.; Kosugi, Y.; et al. SARS-CoV-2 spike L452R variant evades cellular immunity and increases infectivity. *Cell Host Microbe* **2021**, *29*, 1124–1136.e11. [[CrossRef](#)] [[PubMed](#)]
85. Zahradník, J.; Marciano, S.; Shemesh, M.; Zoler, E.; Harari, D.; Chiaravalli, J.; Meyer, B.; Rudich, Y.; Li, C.; Marton, I.; et al. SARS-CoV-2 variant prediction and antiviral drug design are enabled by RBD in vitro evolution. *Nat. Microbiol.* **2021**, *6*, 1188–1198. [[CrossRef](#)] [[PubMed](#)]
86. Suppiah, J.; Kamel, K.A.; Mohd-Zawawi, Z.; Afizan, M.A.; Yahya, H.; Md-Hanif, S.A.; Thayan, R. SHORT COMMUNICATION Phylogenomic analysis of SARS-CoV-2 from third wave clusters in Malaysia reveals dominant local lineage B. 1.524 and persistent spike mutation A701V. *Trop. Biomed.* **2021**, *38*, 289–293. [[CrossRef](#)]

-
87. Fantini, J.; Yahi, N.; Colson, P.; Chahinian, H.; La Scola, B.; Raoult, D. The puzzling mutational landscape of the SARS-2-variant Omicron. *J. Med. Virol.* **2022**, *94*, 2019–2025. [[CrossRef](#)]
 88. Hoffmann, M.; Krüger, N.; Schulz, S.; Cossmann, A.; Rocha, C.; Kempf, A.; Nehlmeier, I.; Graichen, L.; Moldenhauer, A.-S.; Winkler, M.S.; et al. The Omicron variant is highly resistant against antibody-mediated neutralization: Implications for control of the COVID-19 pandemic. *Cell* **2022**, *185*, 447–456.e11. [[CrossRef](#)]